Molecular Crystals and Liquid Crystals

ISSN: 1542-1406 (Print) 1563-5287 (Online) Journal homepage: https://www.tandfonline.com/loi/gmcl20

A density functional theory study on multiple exciton generation in lead chalcogenides

Nur Farha Shaafi, Saifful Kamaluddin Muzakir, Mohd Fakhrul Zamani Kadir & Shujahadeen B. Aziz

To cite this article: Nur Farha Shaafi, Saifful Kamaluddin Muzakir, Mohd Fakhrul Zamani Kadir & Shujahadeen B. Aziz (2019) A density functional theory study on multiple exciton generation in lead chalcogenides, Molecular Crystals and Liquid Crystals, 693:1, 57-65, DOI: 10.1080/15421406.2020.1723919

To link to this article: https://doi.org/10.1080/15421406.2020.1723919

Published online: 02 May 2020.

MOLECULAR CRYSTALS AND LIQUID CRYSTALS
2019, VOL. 693, NO. 1, 57–65
https://doi.org/10.1080/15421406.2020.1723919

Taylor & Francis
Taylor & Francis Group

A density functional theory study on multiple exciton generation in lead chalcogenides

Nur Farha Shaafi[a], Saifful Kamaluddin Muzakir[a], Mohd Fakhrul Zamani Kadir[b], and Shujahadeen B. Aziz[c,d]

[a]Material Technology Programme, Faculty of Industrial Sciences and Technology, Universiti Malaysia Pahang, Lebuhraya Tun Razak, Gambang, Kuantan, 26300, Pahang, Malaysia; [b]Center of Foundation Studies in Science, University of Malaya, 50603 Kuala Lumpur, Malaysia; [c]Advanced Polymeric Materials Research Lab, Department of Physics, College of Science, University of Sulaimani, Qylasan Street, Sulaimani, 46001 Kurdistan Regional Government, Iraq; [d]Komar Research Center (KRC), Komar University of Science and Technology, Sulaimani, 46001, Kurdistan Regional Government, Iraq

ABSTRACT

Quantum confined structure-based solar cell is promising two folds increment of the maximum theoretical photovoltaic conversion efficiency i.e., > 60% in comparison with that of the bulk analogs e.g., silicon-based and dye sensitized solar cell (ca. 32% of maximum theoretical efficiency). The key to the significant increment is the ability of the fluorophore to exhibit multiple exciton generation upon absorption photon with sufficient energy. Small size of lead chalcogenides (PbS, PbSe, PbTe) crystals have been reported and proven experimentally could exhibit this unique property. We have investigated few clusters of narrow bandgap lead chalcogenides nanocrystals i.e., (PbS)*n*, (PbSe)*n* and (PbTe)*n*; which $n = 4$ - 80. The cluster models were optimized using quantum chemical calculations to the lowest energy geometry at B3LYP/lanl2dz level of theory. The predicted realistic $(PbS)_{80}$, $(PbSe)_{50}$, and $(PbTe)_{74}$ clusters with the size, and bandgap of 4.58 nm (2.00 eV), 4.03 nm (1.51 eV), and 4.84 nm (1.55 eV) are smaller than that of their exciton Bohr radius i.e., 5.01, 13.1, and 24.8 nm respectively. Therefore, the occurrence of multi exciton generation in the clusters is hypothesized upon absorption of photon with $E_{photon} = 2E_g$.

KEYWORDS

Density functional theory; lead chalcogenides; multiple exciton generation; quantum confined structure

1. Introduction

Lead chalcogenides (PbS, PbSe, and PbTe) are narrow bandgap semiconducting materials (i.e., 0.37, 0.26, and 0.29 eV respectively) which exhibited interesting properties i.e., high dielectric constant, low resistivity, and large carrier mobility [1]. They have been used intensively for the applications of energy storage [2,3], optoelectronic [4], sensor [5,6] and, photocatalyst [7]. Reduction of size of a semiconducting material (below its exciton Bohr radius) would alter the stated bulk-properties above, and therefore would offer new possibilities of applications. The large exciton Bohr radius of the lead chalcogenides i.e., PbS (5.01 nm), PbSe (13.1 nm), and PbTe (24.8 nm) [8] would offer vast

CONTACT Saifful Kamaluddin Muzakir saifful@Ump.edu.my Material Technology Programme, Faculty of Industrial Sciences and Technology, Universiti Malaysia Pahang, Lebuhraya Tun Razak, Gambang, Kuantan, 26300, Pahang, Malaysia

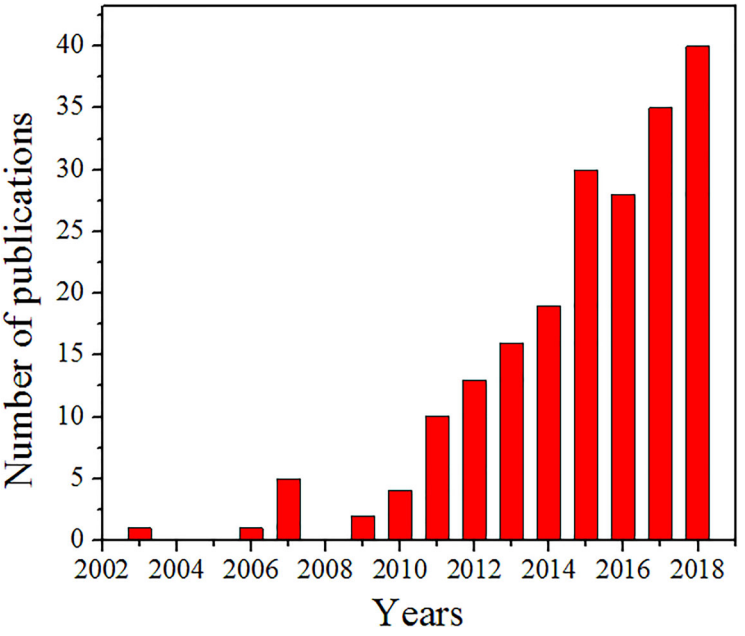

Figure 1. Number of papers published from 2002 to 2018; generated from ISI Web of Science using keywords 'lead chalcogenide' and 'solar cell'.

morphologies of quantum confined materials e.g., quantum dots, nanorods, nanospikes, nanobelts, nanoneedles, nanosheets, nanoflowers etc. The quantum confined lead chalcogenides have been studied extensively in the perspective of their unique properties (i.e., chemical, structural and, electronic) in comparison with that of their bulk counterpart. A specific property of the quantum confined lead chalcogenides which have intrigued researchers in photovoltaic field (Figure 1) - multiple exciton generation (MEG) [9,10]; which would increase the maximum theoretical efficiency of quantum dots solar cell exceeding 60% [11].

The drastic increment of the theoretical efficiency of a quantum confined structure-based solar cell is rooted from peculiar band structure of the quantum confined (QC) fluorophore; which differs from the bulk fluorophore. Expansion of energy levels in a QC fluorophore i.e., the highest occupied molecular orbitals (HOMO), the lowest unoccupied molecular orbitals (LUMO), and the bandgap; has been reported [12–16]. The MEG is a process which yielded more than one exciton upon absorption of single photon (Figure 2a) [17,18]. Upon illumination of photon with energy greater than the bandgap of the QC fluorophore, a ground state electron would absorb the energy, and consequently excited to a higher energy level (e.g., from HOMO -0 to LUMO +1). The excited state electron would undergo a relaxation from LUMO +1 to LUMO +0 which would release the excess of absorbed energy in a form of photon with energy equal or greater than the bandgap. A neighboring electron would absorb the emitted photon, and excited (e.g., from HOMO -0 to LUMO +0); which cumulatively two excited state electron–hole pairs (exciton) are produced upon absorption of single photon. The bulk fluorophore however exhibits continuous energy band structure (Figure 2b). An excited state electron that

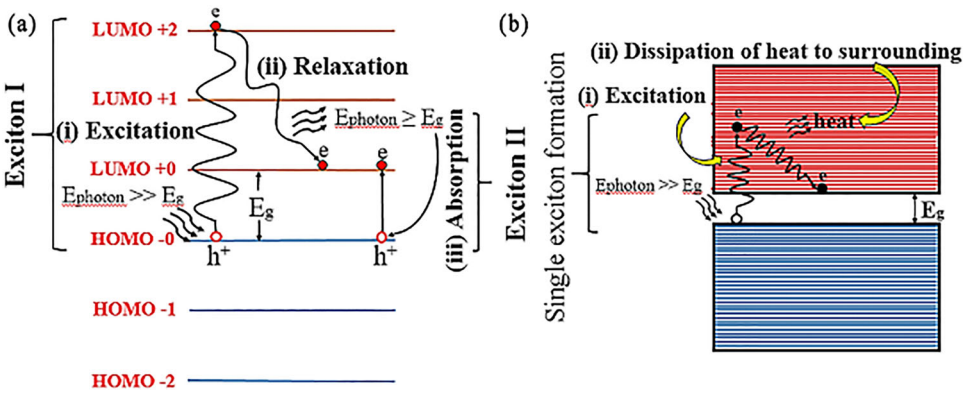

Figure 2. (a) The MEG in QCS fluorophore upon absorption of photon with $E_{photon} \gg Eg$ which involves (i) excitation of a ground state electron, (ii) relaxation to the lowest unoccupied energy level with subsequent photon emission, and (iii) absorption of the photon by neighboring electron, and subsequent second electron excitation. (b) Dissipation of excess energy of an excited state electron during relaxation to the lowest conduction band in bulk fluorophore.

undergoes a relaxation mechanism would only emit heat; which later will be dissipated to the surroundings [19] and would not contribute to excitation of neighboring electron.

A correlation between quantum efficiency (QE) and energy of absorbed photon in lead chalcogenides has been established. The correlation has revealed critical requirements for the MEG to occur in QC lead chalcogenides i.e., threshold value of QE ca. 300%, and $E_{photon} = 2E_g$ [12,20]. A specific chemical structure of the QC lead chalcogenides that would exhibit MEG however has not been revealed to date.

Quantum chemical calculations under the framework of density functional theory (DFT) have received intense focus owing to its ability to calculate the ground state, excited state, and emitting state properties of materials accurately [21]. We have successfully established and validated few QC's in our previous works in quantum dots solar cell (QDSC) which have contributed to the revelation of six detrimental effects during device fabrications [22]. Similar approach is aimed in this work which would yield some insightful findings.

2. Methodology

The ground state geometry models of the lead chalcogenides were built based on their well-established bulk crystallographic profiles. The models later undergo series of calculations to optimize their internal coordinates (i.e., bond lengths, bond angles, and dihedral angles) to the lowest energy structure; which the interactions (potential and kinetic energy) between electron, proton, and neutron, and correlation-exchange energy between two neighboring electrons in same orbital are taken into considerations [23]. Models that meet convergence requirements for minimum energy structure then validated as realistic upon convergence in harmonic frequency calculations – exhibit only positive vibrational modes [24]. All theoretical calculations were made using Becke's three parameter hybrid method with Lee, Yang and Parr (B3LYP) correlation functional [12,25,26], and lanl2dz basis set; which provides accurate description of binding energy,

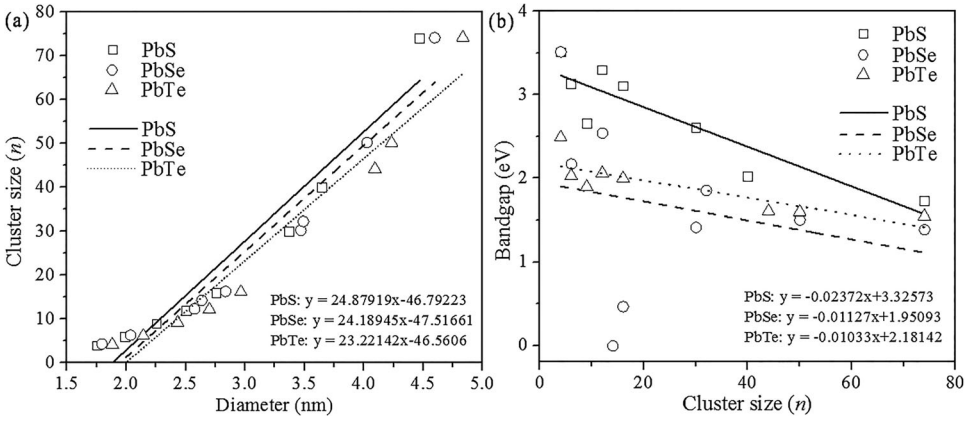

Figure 3. Predictions of (a) cluster size, and (b) energy bandgap of (PbS)*n*, (PbSe)*n* and (PbTe)*n*. The straight lines are fitted data.

surface states, trap states and surface stabilization [27]. The excited state properties of the clusters i.e., the HOMO, LUMO, and bandgap were determined using time-dependent density functional theory (TD-DFT) calculations upon validation of realistic clusters.

3. Results and discussions

3.1. Determination and validation of (PbX)n realistic clusters

Luque et. al (2007) have investigated the correlation between the QE, MEG and bandgap of PbS, PbSe, and PbTe using a mid-infrared probe. An observation of high QE ca. 300% indicated that occurrence of MEG (ca. Three excitons per absorbed photon) which only could be demonstrated in PbS, PbSe, and PbTe with specific bandgap viz., 0.8, 0.91, dan 0.91 eV; with corresponding size viz., 5.5, 3.9, and 5.5 nm respectively. The specified sizes therefore were used as main reference in our work – modeling realistic clusters of PbS, PbSe, and PbTe which would demonstrate the MEG. Several cluster models of (PbX)*n* (with X = S, Se, and Te, and *n* = 4-80) were built based on well-established crystallographic profiles of bulk lead chalcogenides [28–31].

The models were validated as realistic cluster using procedure mentioned in previous section. The size (diameter) of the realistic clusters was calculated based on their volume using polarizable continuum model (PCM). Figure 3a shows that the diameter increases with increment of number of atoms arranged in each cluster model.

The (PbS)*n*, (PbSe)*n*, and (PbTe)*n* clusters with specific number of atoms which would exhibit the targeted size have been predicted using the following equations:

$$Clustersize(n)of\,PbS = (24.87921)x - 46.79226 \quad (1)$$

$$Clustersize(n)of\,PbSe = (24.18952)x - 47.51679 \quad (2)$$

$$Clustersize(n)of\,PbTe = (23.2213)x - 46.56047 \quad (3)$$

The targeted size of PbS (5.5 nm), PbSe (3.9 nm), and PbTe (5.5 nm) was substituted in Equation 1–3, therefore concluded cluster size (*n*) of 90, 47, and 80 for PbS, PbSe,

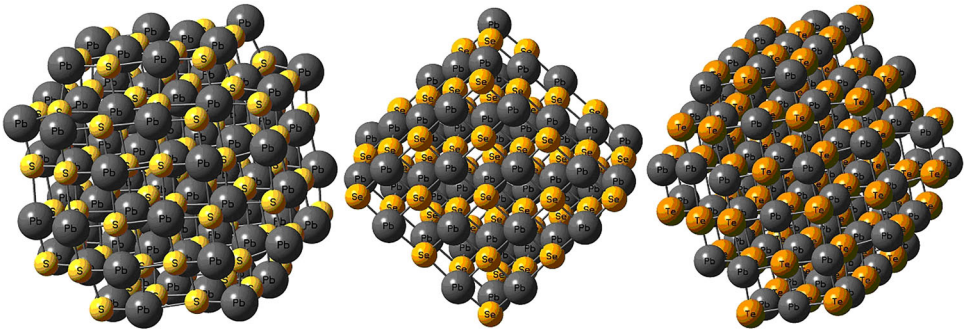

Figure 4. (From left) Optimized structures of $(PbS)_{80}$, $(PbSe)_{50}$, and $(PbTe)_{74}$; validated as realistic clusters.

Table 1. The calculated E_g of the realistic clusters.

Cluster	E_g (Equation 4–6)	E_g (TD-DFT)
$(PbS)_{80}$	1.43 eV	2.00 eV
$(PbSe)_{50}$	1.39 eV	1.51 eV
$(PbTe)_{74}$	1.42 eV	1.55 eV

and PbTe respectively. However, upon fulfillment of strict requirement of convergence, we have successfully validated realistic clusters with n that are in good agreement with that of the predicted clusters i.e., $(PbS)_{80}$, $(PbSe)_{50}$, and $(PbTe)_{74}$ (Figure 4). These three clusters exhibited size of 4.58, 4.03, and 4.84 nm respectively which supports the findings by Luque et al. (2007).

3.2. The MEG occurrence in the realistic clusters

The excited state properties of the realistic $(PbS)_{80}$, $(PbSe)_{50}$, and $(PbTe)_{74}$ clusters were calculated using TD-DFT. Their bandgaps (Table 1) are in good agreement with that of the prediction made based on Figure 3b using the following equations:

$$Eg_{PbS} = (-0.02372)x + 3.32573 \quad (4)$$

$$Eg_{PbSe} = (-0.01127)x + 1.95093 \quad (5)$$

$$Eg_{PbTe} = (-0.01033)x + 2.18142 \quad (6)$$

The excited state energy levels of the realistic clusters were analyzed based on minimum requirement of MEG in lead chalcogenides viz., $E_{photon} = 2E_g$. An electron excitation upon absorption of photon with such energy would happen from the ground state (with negative energy level) to the excited state with negative energy level – known as bonding energy level. The highly energized electron would undergo a relaxation to the lowest excited state energy level. Subsequently, a photon would be emitted, and later absorbed by a neighboring electron that lead to formation of second exciton (MEG is favored). The electron transitions from the ground state to the excited state, and MEG occurrence in the realistic clusters are summarized in Table 2. The MEG is likely to occur in the predicted realistic clusters of $(PbS)_{80}$, $(PbSe)_{50}$, and $(PbTe)_{74}$, along with

Table 2. Electron transitions from the ground (GS) to the excited (ES) states in the realistic clusters; which would favor MEG occurrence (MEG) upon absorption of $E_{photon} = 2E_g$.

Size (*n*)	Property	(PbS)*n*		(PbSe)*n*		(PbTe)*n*	
4	GS	HOMO-0	(-7.17 eV)	HOMO-0	(-7.17 eV)	HOMO-0	(-5.93 eV)
	ES	LUMO + 12	(+2.26 eV)	LUMO + 12	(+1.86 eV)	LUMO + 12	(+1.16 eV)
	MEG	Unlikely		Unlikely		Unlikely	
6	GS	HOMO-0	(-5.86 eV)	HOMO-0	(-5.90 eV)	HOMO-0	(-5.78 eV)
	ES	LUMO + 17	(+0.41 eV)	LUMO + 17	(+0.76 eV)	LUMO + 18	(+0.13 eV)
	MEG	Unlikely		Unlikely		Unlikely	
9	GS	HOMO-0	(-6.83 eV)	NON-REALISTIC		HOMO-0	(-5.70 eV)
	ES	LUMO + 17	(+0.41 eV)			LUMO + 22	(+0.02 eV)
	MEG	Unlikely				Unlikely	
12	GS	HOMO-0	(-7.02 eV)	HOMO-0	(-6.00 eV)	HOMO-0	(-5.80 eV)
	ES	LUMO + 36	(+1.67 eV)	LUMO + 32	(+1.00 eV)	LUMO + 25	(-0.79 eV)
	MEG	Unlikely		Unlikely		Likely	
16	GS	HOMO-0	(-6.94 eV)	HOMO-0	(-5.87 eV)	HOMO-0	(-5.80 eV)
	ES	LUMO + 48	(+1.67 eV)	LUMO + 30	(-0.62 eV)	LUMO + 17	(-0.19 eV)
	MEG	Unlikely		Likely		Likely	
30	GS	HOMO-0	(-6.78 eV)	HOMO-0	(-4.06 eV)	NON-REALISTIC	
	ES	LUMO + 73	(+0.77 eV)	LUMO + 52	(-0.30 eV)		
	MEG	Unlikely		Likely			
32	GS	NON-REALISTIC		HOMO-0	(-5.72 eV)	NON-REALISTIC	
	ES			LUMO + 71	(-0.05 eV)		
	MEG			Likely			
40	GS	HOMO-0	(-6.67 eV)	NON-REALISTIC		NON-REALISTIC	
	ES	LUMO + 67	(-2.63 eV)				
	MEG	Likely					
44	GS	NON-REALISTIC		NON-REALISTIC		HOMO-0	(-5.62 eV)
	ES					LUMO + 89	(-0.96 eV)
	MEG					Likely	
50	GS	NON-REALISTIC		HOMO-0	(-5.54 eV)	HOMO-0	(-4.02 eV)
	ES			LUMO + 82	(-0.62 eV)	LUMO + 90	(-5.54 eV)
	MEG			Likely		Likely	
74	GS	HOMO-0	(-6.54 eV)	HOMO-0	(-5.56 eV)	HOMO-0	(-5.62 eV)
	ES	LUMO + 65	(-3.08 eV)	LUMO + 58	(-2.77 eV)	LUMO + 87	(-2.52 eV)
	MEG	Likely		Likely		Likely	
80	GS	HOMO-0	(-6.70 eV)	NON-REALISTIC		NON-REALISTIC	
	ES	LUMO + 89	(-0.10 eV)				
	MEG	Likely					

few other clusters viz., $(PbS)_{74}$, $(PbS)_{40}$, $(PbSe)_{74}$, $(PbSe)_{32}$, $(PbSe)_{30}$, $(PbSe)_{16}$, $(PbTe)_{50}$, $(PbTe)_{44}$, $(PbTe)_{16}$, and $(PbTe)_{12}$.

However, an electron transition from the ground state (with negative energy level) to the excited state with positive energy level – known as anti-bonding energy level; would contribute insignificantly to the MEG mechanism. The absorbed photon with $E_{photon} = 2E_g$ is sufficient to liberate the electron from the unoccupied molecular orbitals; therefore, the highly energized electron would not undergo the relaxation to the lowest excited state energy level. The MEG is unlikely to occur in few realistic clusters viz., $(PbS)_{30}$, $(PbS)_{16}$, $(PbS)_{12}$, $(PbS)_9$, $(PbS)_6$, $(PbS)_4$, $(PbSe)_{12}$, $(PbSe)_6$, $(PbSe)_4$, $(PbTe)_9$, $(PbTe)_6$, and $(PbTe)_4$.

3.3. The trend of MEG occurrence in $(PbS)_{80}$, $(PbSe)_{50}$ and $(PbTe)_{74}$

The absorption spectra of the $(PbS)_{80}$, $(PbSe)_{50}$ and $(PbTe)_{74}$ clusters were calculated using TD-DFT; and subsequently the E_g of the clusters was determined using Tauc's

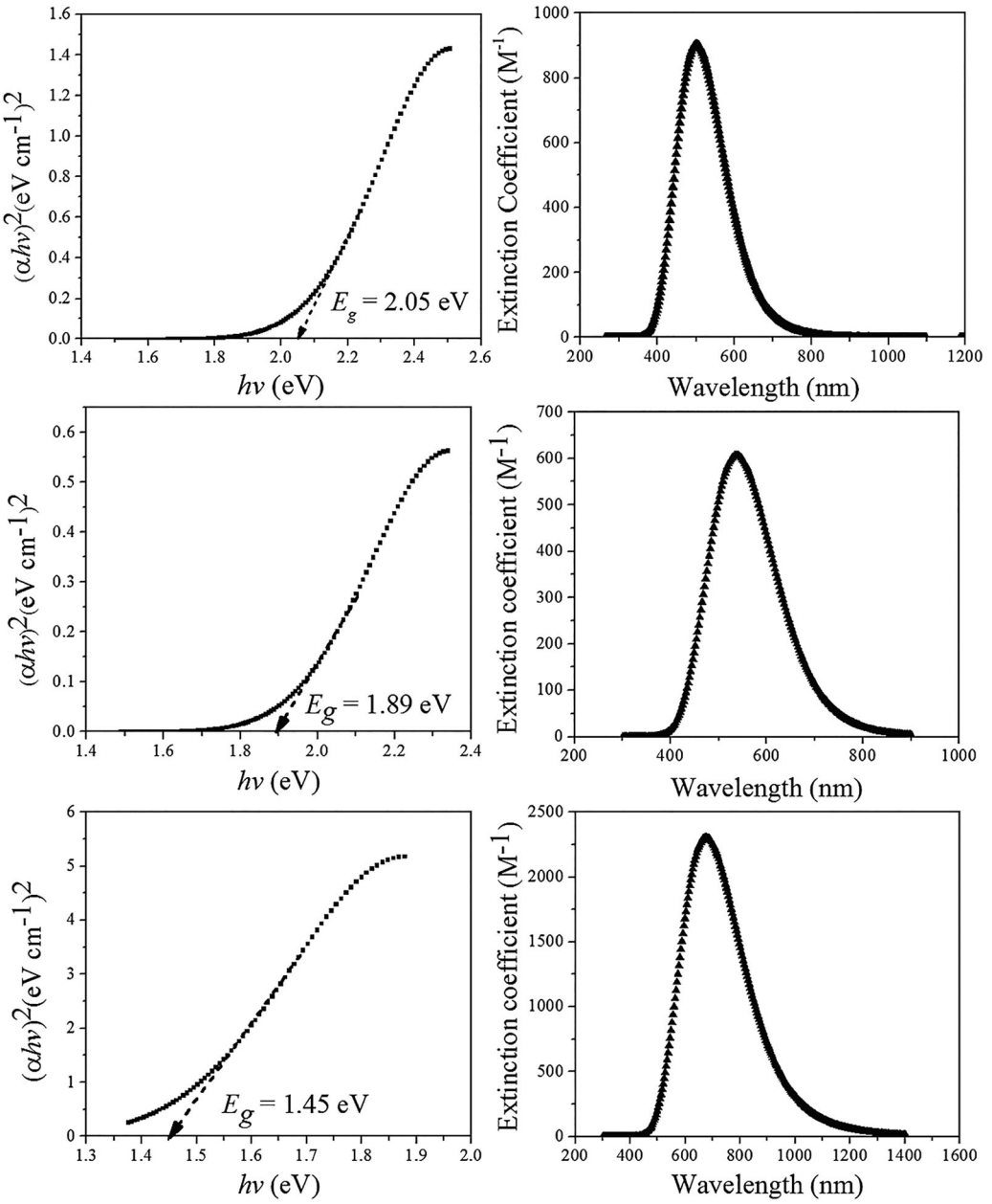

Figure 5. (Left) The Tauc's Plot of (from top to bottom) $(PbS)_{80}$, $(PbSe)_{50}$, and $(PbTe)_{74}$. (Right) extinction coefficient of the clusters (from top to bottom) respectively.

plot (Figure 5). The E_g of 2.05, 1.89 and 1.45 eV respectively were shown, which in acceptable agreement with the E_g determined in Table 1. The wavelength which correspond to photon with energy of $2E_g$ (threshold energy to initiate MEG) was calculated using the formula:

$$\lambda_{2Eg} = hc/2_{Eg} \tag{7}$$

where the speed of light, c is 3.00×10^8 m/s and the Planck's constant, h is 4.14×10^{-15} eV.s; yielded the λ_{2Eg} requirement for $(PbS)_{80}$, $(PbSe)_{50}$ and $(PbTe)_{74}$ viz., ca. 434, 447, and 437 nm respectively. The strength of photon absorption by the clusters was analyzed based on the extinction coefficient-wavelength graphs (Figure 5); which showed that the determined wavelengths are in the active-absorption range (positive value of extinction coefficient). However, a constant decrement of extinction coefficient with increment of molecular weight is observed i.e., 387.83 (PbS), 166.88 (PbSe), and 6.78 M^{-1} (PbTe). The lower the extinction coefficient at specific wavelength, the weaker the clusters would absorb the photon correspond to the wavelength. Therefore, concludes that the possibility of occurrence of MEG in the clusters would be decreased following the trend viz., $(PbS)_{80} > (PbSe)_{50} > (PbTe)_{74}$.

4. Conclusions

In conclusion, realistic clusters of $(PbS)_{80}$, $(PbSe)_{50}$, and $(PbTe)_{74}$ with bandgap of 2.00, 1.51, and 1.55 eV respectively have been established using series of quantum chemical calculations. The ground, and excited state properties of the clusters were studied; which clearly showed that the MEG could happen upon absorption of photon with $E_{photon} = 2E_g$ i.e., in the region of violet and blue light. The photon absorption properties of the clusters were examined, showed that the blue and violet light are in the active-absorption range of the clusters. However, the extinction coefficient at the specific wavelength degraded with the trend of $(PbS)_{80} > (PbSe)_{50} > (PbTe)_{74}$; which denote decreasing possibility of occurrence of the MEG.

Acknowledgments

This work is funded by the Research & Innovation Department of Universiti Malaysia Pahang, and the Ministry of Education of Malaysia through the Fundamental Research Grant Scheme (RDU 150111) and Postgraduate Research Scheme (PGRS190346).

References

[1] D. C. Gupta and I. H. Bhat, *J. Mol. Model.* **19** (9), 3481 (2013). doi:10.1007/s00894-013-1870-4
[2] G. Chen *et al.*, *Chem. Soc. Rev.* **42** (21), 8304 (2013). doi:10.1039/c3cs60054h
[3] H. Lee *et al.*, *Adv. Funct. Mater.* **19** (17), 2735 (2009). doi:10.1002/adfm.200900081
[4] D. V. Talapin *et al.*, *Chem. Rev.* **110** (1), 389 (2010). doi:10.1021/cr900137k
[5] H. Zogg *et al.*, *Semicond. Sci. Technol.* **6** (12C), C36 (1991). doi:10.1088/0268-1242/6/12C/008
[6] S. Liu, and Z. Tang, *J. Mater. Chem.* **20** (1), 24 (2010). doi:10.1039/B911328M
[7] L. N. Qiao *et al.*, *AIP. Adv.* **6** (1), 015108 (2016).
[8] W. Ma *et al.*, *Nano Lett.* **9** (4), 1699 (2009). doi:10.1021/nl900388a
[9] R. D. Schaller and V. I. Klimov, *Phys. Rev. Lett.* **92** (18), 186601 (2004). doi:10.1103/PhysRevLett.92.186601
[10] L. W. Wang *et al.*, *Phys. Rev. Lett.* **91** (5), 056404 (2003). doi:10.1103/PhysRevLett.91.056404
[11] J. E. Murphy *et al.*, *J. Am. Chem. Soc.* **128**, 3241 (2006). doi:10.1021/ja0574973
[12] J. E. Murphy *et al.*, *J. Am. Chem. Soc.* **128** (10), 3241 (2006). doi:10.1021/ja0574973

[13] L. E. Brus, *J. Chem. Phys.* **80** (9), 4403 (1984). doi:10.1063/1.447218
[14] A. L. Efros and A. Efros, *Sov. Phys. Semicond.* **16**, 772 (1982).
[15] A. P. Alivisatos, *J. Phys. Chem.* **100** (31), 13226 (1996). doi:10.1021/jp9535506
[16] Y. Wang and N. Herron, *J. Phys. Chem.* **95** (2), 525 (1991). doi:10.1021/j100155a009
[17] M. C. Beard *et al.*, *Acc. Chem. Res.* **46** (6), 1252 (2013). doi:10.1021/ar3001958
[18] W. Shockley and H. J. Queisser, *J. Appl. Phys.* **32** (3), 510 (1961). doi:10.1063/1.1736034
[19] M. C. Beard *et al.*, *Phil. Trans. R Soc. A* **373** (2044), 20140412 (2015). doi:10.1098/rsta.2014.0412
[20] R. J. Ellingson *et al.*, *Nano Lett.* **5** (5), 865 (2005). doi:10.1021/nl0502672
[21] W. Koch, M. C. Holthausen, and M. C. Holthausen, *Accounts of chemical research* (Weinheim: Wiley-Vch, 2001).
[22] S. K. Muzakir *et al.*, *Phys. Chem. Chem. Phys.* **15** (38), 16275 (2013). doi:10.1039/c3cp52858h
[23] B. J. Brune *et al.*, *Langmuir* **15** (11), 3987 (1999). doi:10.1021/la990091h
[24] N. S. Abraham and M. R. Shirts, *J. Chem. Theory Comput.* **14** (11), 5904 (2018). doi:10.1021/acs.jctc.8b00460
[25] R. D. Schaller and V. I. Klimov, *Nano Lett.* **5** (5), 865 (2004). doi:10.1021/nl400141w
[26] J. A. Mcguire *et al.*, *Acc. Chem. Res.* **41** (12), 1810 (2008). 10.1021/ar800112v
[27] P. J. Hay and W. R. Wadt, *J. Chem. Phys.* **82** (1), 270 (1985). doi:10.1063/1.448799
[28] V. F. Skums, R. L. Pink, and M. R. Allazov, *J. Inorg. Mater.* **27** (8), 1336 (1991).
[29] T. Chattopadhyay *et al.*, *Phys. B Condens. Matter* **139**, 356 (1986). doi:10.1016/0378-4363(86)90598-X
[30] V. Leute and N. Volkmer, *Int. J. Phys. Chem. Chem. Phys.* **144** (144), 145 (1985). doi:10.1524/zpch.1985.144.144.145
[31] A. Luque, A. Martí, and A. J. Nozik, *MRS Bull.* **32** (3), 236 (2007). doi:10.1557/mrs2007.28